A New Strategy for the Preparation of Peptide-Targeted Radiopharmaceuticals Based on an Fmoc-Lysine-Derived Single Amino Acid Chelate (SAAC). Automated Solid-Phase Synthesis, NMR Characterization, and in Vitro Screening of fMLF(SAAC)G and fMLF[(SAAC−Re(CO)$_3$)$^+$]G

Karin A. Stephenson,[†] Jon Zubieta,[‡] Sangeeta Ray Banerjee,[‡] Murali K. Levadala,[‡] Linda Taggart,[†] Lorna Ryan,[†] Nicole McFarlane,[†] Douglas R. Boreham,[†] Kevin P. Maresca,[§] John W. Babich,[§] and John F. Valliant*[,†]

Department of Chemistry and The Medical Physics and Applied Radiation Sciences Unit, McMaster University, Hamilton, ON, Canada L8S 4M1, Department of Chemistry, Syracuse University, Syracuse, New York 13244-4100, and Molecular Insight Pharmaceuticals Inc., Cambridge, Massachusetts 02142. Received July 21, 2003; Revised Manuscript Received October 12, 2003

A tridentate single amino acid chelate (SAAC) derived from N-α-Fmoc-L-lysine was incorporated within a short peptide sequence using an automated peptide synthesizer. Novel derivatives of the chemotactic peptide fMLF were prepared such that the SAAC and its Re complex were selectively placed between a terminal glycine amino acid and the targeting fMLF sequence. The products, which were synthesized in parallel, were characterized by mass spectrometry and multi-NMR spectroscopy. The latter technique demonstrated that the structures of the targeting portions of the peptides are the same in the SAAC and Re−SAAC derivatives. The affinities of the reported compounds for the formyl peptide receptor were subsequently determined using flow cytometry and were found to be comparable to that of the parent peptide. The results of this work demonstrate the feasibility and numerous benefits of using the SAAC system to prepare peptide-targeted Tc(I) and Re(I) radiopharmaceuticals.

INTRODUCTION

Small peptides have proven to be one of the most effective means of targeting radionuclides to specific receptors (*1*). The success of peptides as biological vectors for radioisotopes is a result of their receptor specificity, ease of preparation and modification, ability to target receptors, and clearance from nontarget tissues in a time frame that correlates with the half-life of clinically useful radionuclides such as ^{99m}Tc, ^{111}In, and ^{18}F.

It has been well-documented that several factors influence the receptor binding affinity and biodistribution of technetium-labeled peptides (*2*). These include the site of derivatization, the presence and type of a spacer group between the ligand−metal complex and the peptide, and the nature of the Tc−ligand complex (charge, size, lipophilicity, etc.). As a means of identifying optimal combinations of these factors several groups have begun to employ solid-phase synthesis (SPS) strategies. SPS is attractive because it is a convenient means of preparing analogues of a particular peptide−ligand bioconjugate in parallel (*3*).

The most common SPS strategy used to prepare peptide-targeted Tc radiopharmaceuticals has been to append Tc ligands to the N-termini of peptides bound to a polymeric support. Hoffman et al., for example, reported the synthesis of a series of bombesin derivatives in which a N_3S triamide chelate and its Re complex were linked to the resin-bound peptide through a variety of different spacer groups (*4*). Gariépy and co-workers described a related solid-phase synthesis method for adding a diaminedithiol ligand to the N-terminus of short peptides (*5*). Blower and co-workers recently described a novel SPS approach in which a hydrazinonicotinyl acid (HYNIC) derivative of Fmoc-lysine was used as a metal-binding amino acid analogue (*6*, *7*). The N-protected HYNIC derivative was successfully incorporated within a bioactive peptide using standard Fmoc solid-phase peptide chemistry.

The above-mentioned SPS methods have some limitations including one or more of the following: a lack of flexibility in terms of changing the site of derivatization, the need to employ additional protecting groups on the ligand donor atoms, the inability to prepare the corresponding Re or ^{99}Tc complexes on the solid support and/or in solution and the need to use HPLC to obtain products of sufficient purity. The ideal SPS strategy should be based on a ligand system that forms stable and/or inert complexes with Tc/Re and, like the HYNIC system reported by Blower et al., is able to be incorporated into a peptide at any position using conventional SPS methods. The SPS strategy should also allow the ligand to be incorporated into the peptide without the need for additional protecting groups and isolation of the bioconjugate should be accomplished without the need for extensive HPLC purification. The Re (or ^{99}Tc) complex of the ligand should be sufficiently stable and well-defined to permit the synthesis of the metal complex of

* To whom correspondence should be addressed: Tel: 905-525-9140 ext. 23303 (J.F.V.); FAX: 905-522-2509; E-mail: valliant@mcmaster.ca.

[†] McMaster University, Hamilton, Ontario, Canada.

[‡] Syracuse University, Syracuse, NY.

[§] Molecular Insight Pharmaceuticals Inc., Cambridge, MA.

10.1021/bc034128s CCC: $27.50 © 2004 American Chemical Society
Published on Web 11/22/2003

the peptide using the same solid-phase synthetic methodology used to prepare the ligand. At present, Re and ^{99}Tc complexes are often prepared separately for characterization purposes, in vitro screening experiments and to verify the nature of products produced at the tracer level. To consider using combinatorial chemistry and high throughput screening methods as a means of identifying novel radiopharmaceuticals, a viable SPS method should allow for the Re and/or ^{99}Tc peptide complex to be prepared in parallel with the free ligand.

The ability to meet these criteria depends greatly upon the choice of ligand. Zubieta and co-workers recently described the synthesis and structural characterization of a series of Re(I) complexes of tridentate chelates containing two pyridine and one tertiary amine donor groups (*8*). The ligands and their Re(I) complexes, which were prepared in high yield, are stable to a wide range of reaction conditions making them ideal synthons for solid-phase peptide synthesis. With this in mind, an analogous ligand was prepared from Fmoc-lysine, which is herein referred to as a single amino acid chelate (SAAC). The SAAC is a unique Re(I)/Tc(I)-binding amino acid mimic, which has the potential to be incorporated into a peptide at any position using standard automated synthetic protocols. The corresponding Re complex, owing to its stability, inertness, and well-defined structure, should similarly be capable of being incorporated into a peptide using the same basic synthetic procedure. We report herein, the preparation, characterization, and in vitro screening studies of SAAC and Re−SAAC-peptide derivatives prepared using a convenient automated solid-phase synthesis methodology.

EXPERIMENTAL PROCEDURES

Materials. Unless otherwise stated, all reagents and solvents were ACS grade or higher and used without further purification from commercial suppliers. Polystyrene-based *N*-α-9-fluorenylmethoxycarbonyl (Fmoc)-glycine loaded SASRIN resin (0.69 mmol g-1, 1% divinylbenzene, 200−400 mesh) was obtained from Bachem Inc. Fmoc-protected amino acids were purchased from Nova-Biochem Inc., Bachem Inc., and Advanced ChemTech Inc. Fluorescein-labeled fNLFNTK was purchased from Molecular Probes Inc. (product # F-1314).

Instrumentation. All peptides were prepared on an Advanced ChemTech 348 Ω Peptide Synthesizer using a 40 well reaction vessel. Peptides were analyzed by electrospray mass spectrometry using a Micromass Quattro Ultima instrument in positive ion mode. Samples were dissolved in 50/50 ACN/H_2O prior to analysis. FTIR spectra were acquired on a Bio-Rad FTS-40 FTIR spectrometer. NMR experiments were performed using a Bruker Avance DRX-500 NMR spectrometer. Proton spectra were acquired at 500.13 MHz using a 5-mm broadband inverse probe with triple axis gradient capability. Spectra were obtained in eight scans in 32K data points over a 6.775 kHz spectral width (2.418 s acquisition time). Proton COSY 2-D NMR spectra were recorded in the absolute value mode using the pulse sequence 90°−t1−45°-acq and included pulsed field gradients for coherence selection. During 2-D Fourier transformation a sine-bell squared window function was applied to both dimensions. The transformed data were then symmetrized. Carbon-13 NMR spectra were recorded at 125.771 MHz using the 5 mm broadband inverse probe with triple axis gradient capability. The spectra were acquired over a 28.986 kHz spectral width in 32K data points (0.565 s acquisition time). Inverse detected ^{1}H−^{13}C 2-D chemical shift correlation spectra were acquired in the phase-sensitive mode using the pulsed field gradient version the HSQC pulse sequence. Inverse detected ^{1}H−^{13}C 2-D chemical shift correlation spectra through two- and three-bond coupling interactions were acquired in the absolute value mode using the pulsed field gradient version of the HMBC pulse sequence. ROESY 2-D spectra were acquired in the phase sensitive mode. The data were acquired in 16 scans for each of the 256 FIDs that contained 2K data points in the F2 dimension over a 3.931 kHz spectral width. Zero-filling in the F1 dimension produced a 1K × 1K data matrix with a digital resolution of 3.839 Hz/point in both dimensions. During the real 2-D Fourier transformation, a sine-bell squared window function shifted by $\pi/2$ was applied to both dimensions. The transformed data were not symmetrized. The ROESY 2-D spectrum was plotted displaying negative contours only. Selective 1-D TOCSY ^{1}H NMR spectra were recorded over a 4.006 kHz spectral width in 32K data points (4.089 s acquisition time). Gaussian-shaped pulses were defined by 256 data points with the pulse being truncated at 1% of the maximum pulse amplitude.

Analytical HPLC was performed using a Varian Pro Star model 330 PDA detector, model 230 solvent delivery system and a C-18 Microsorb column (4.6 × 250 mm, 300 Å-5 μm). Semipreparative HPLC was carried out using a Varian Pro Star HPLC fitted with a model 320 UV-detector, a model 215 solvent delivery system and a C-18 Microsorb column (10 × 250 mm, 300 Å-5 μm). The elution protocol for both analytical and semipreparative experiments was a linear gradient of 25% acetonitrile containing 0.1% TFA to 75% acetonitrile containing 0.1% TFA over 15 min. The flow rates were 1.0 mL min^{-1} and 4.2 mL min^{-1} for the analytical and semipreparative experiments, respectively. All analytical HPLC experiments were monitored at $\lambda = 254$ and 214 nm.

Solid-Phase Peptide Synthesis. Fmoc-glycine-loaded SASRIN resin (300 mg, 0.69 mmol/g) was added to two wells of the reaction vessel, suspended in DMF (2 mL/well) and shaken at 900 rpm for 1 min. The wells were subsequently filtered, suspended in THF (2 mL/well), shaken at 900 rpm for 1 min, and drained for 90 s. The THF wash was repeated two more times. The DMF wash was then repeated a final two times to complete the general wash cycle. This procedure was used between every deprotection and coupling step. Fmoc deprotection was brought about through the addition of 25% v/v piperidine−DMF solution to the active vessels (2 mL/well) and shaking for 5 min at 900 rpm. Following filtration, the process was repeated, shaking for 10 min. The deprotected resin-bound amino acid was washed using the general wash procedure and subsequently coupled to the next Fmoc-protected amino acid using a standard HBTU coupling technique. Coupling reactions initially involved adding DMF (200 μL) to the active vessels followed by the addition of a 4-fold excess of the protected amino acid as a 0.5 M solution in DMF. Four equivalents of HBTU as a 0.5 M solution in DMF was then added followed by a 8-fold excess of DIPEA as 2.0 M solution in DMF. The reaction block was subsequently shaken for 80 min at 900 rpm. Following filtration, the resin was washed using the general washing procedure prior to the start of the next cycle. Peptides were cleaved from the resin support using a TFA cocktail containing EDT (2%), water (2%), and TIS (2%). The cleavage cocktail, cooled to 0 °C, was added to the resin and the mixture allowed to warm to room temperature over 60 min. The suspension was filtered into cold diethyl ether and the resulting heterogeneous solution centrifuged at

Scheme 1. Preparation of SAAC (2) and [SAAC−Re(CO)$_3$]$^+$ (3)

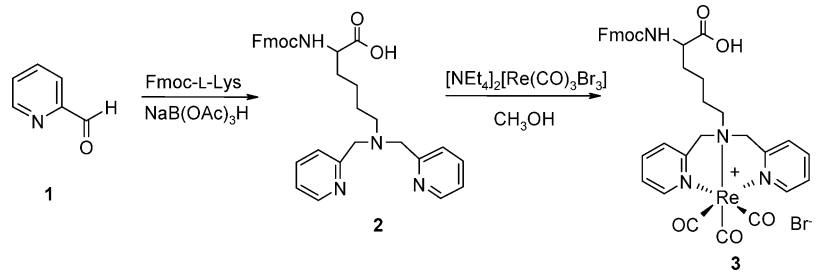

3000 rpm and −5 °C for 10 min. The resulting pellet was washed with cold diethyl ether (3 × 25 mL), dissolved in distilled−deionized water, and lyophilized yielding a white solid for both compounds **6** and **8** (Schemes 2 and 3). Compound **6** showed: FT-IR (KBr, cm^{-1}): 1540 (C═O), 1670 (C═O), 2927 (C−H), and 3069 (N−H); ESMS 805 [M + H]$^+$. Compound **8** showed: FT-IR (KBr, cm-^{1}): 1538 (C═O), 1927 and 2032 (C≡O), 2926 (C−H); ESMS 1075 [M + H]$^+$.

Leukocyte Preparation. Whole human blood (10−15 mL) was collected in vacutainer tubes (Becton Dickinson) containing sodium heparin. The red blood cells were lysed using a modified ammonium chloride method (1 part whole blood to 23 parts 0.145 M ammonium chloride solution containing 1.5 mM potassium bicarbonate and 0.1 mM EDTA). Tubes were incubated at room temperature for 15 min and then centrifuged in a Beckman Coulter Allegra 6R centrifuge at 900 rpm (400 g) for 7 min at 5 °C. The supernatant was removed and the pellet of leukocytes subsequently resuspended in HBSS containing 0.1% BSA, 10 mM HEPES, and 1.5 mM $CaCl_2$ (HBSS+). The cells were spun for 7 min at 400*g* at 5 °C, the supernatant removed, and the pellet resuspended in HBSS+. Cell counts were performed using a hemacytometer and a Beckman Coulter Z2 Coulter Particle Count and Size Analyzer. Cell concentrations were adjusted to 2 × 10^6 mL^{-1}.

Flow Cytometry. Samples were run on a Beckman Coulter EPICS XL, equipped with an argon laser (488 nm excitation wavelength). Fluorescence was measured using a 525 ± 15 nm band-pass filter. The flow cytometer was calibrated with fluorescein isothiocyanate (FITC)-labeled beads (Quantum 26 Beads, Bangs Laboratories, Inc, Fishers, IN) prior to sample analysis. The fluorescence intensity of the standard was provided by the manufacturer in units of Molecules of Equivalent Soluble Fluorochrome (MESF) and ranged from 5300 to 468 800. A linear fit of MESF versus mean channel number of the beads was used to convert all subsequent mean channel values to MESF values.

Equilibrium Binding Assay. The equilibrium-binding assay was used to determine the number of formyl peptide receptors (FPRs) on the surface of the neutrophils and the dissociation constant (K_d) of the fluorescein-labeled fNLFNTK (Molecular Probes) (1.0 nM) by preparing a saturated binding curve of peptide concentrations verses fluorescence intensity. Peptide stock solutions were made by dissolving the peptide derivatives **6** and **8** in DMSO and then diluting with HBSS+ to the desired concentrations, ensuring the concentration of DMSO was less than 0.1%. Cells at 1 × 10^6 mL^{-1} were equilibrated with 0.25, 0.50. 1.0, 3.0, 5.0, 10.0, and 20.0 nM solutions of the peptide derivatives (U) in duplicate. The samples were incubated for 2 h at 0 °C in the dark and then run on the flow cytometer. Neutrophils were gated on the basis of forward and side scatter parameters using Expo 32 ADC software (Beckman Coulter). All samples were repeated in the presence of 30 μM fMLF to account for nonspecific binding. The number of receptor−ligand complexes per cell (B) was determined using the following equation, where Q is a normalization factor used by Waller et al. (*14*) and F is the total fluorescence per cell:

$$B(\text{in ligand bound per cell}) = F\left(\frac{\text{MESF}}{\text{cell}}\right) \times Q$$

The level of nonspecific binding did not vary significantly with concentration of labeled peptide, thus an average value of nonspecific binding was subtracted from the total fluorescence per cell, F, when determining the number of receptor−ligand complexes. The total number of *N*-formyl peptide receptors, R_{tot}, and the equilibrium dissociation constant, K_d, were evaluated by minimizing the squared residual of the equilibrium solution using a one-site binding model (see the following equation). The values of R_{tot} and K_d for each donor were solved simultaneously.

$$[\text{LR}] = \frac{R_{\text{tot}}[\text{L}]}{[\text{L}] + K_d}$$

RESULTS

SAAC Synthesis. The synthesis of the Fmoc-protected single amino acid chelate **2** (Scheme 1) will be described elsewhere (*9*). Briefly, Fmoc-L-lysine was reacted with 2-pyridinecarboxaldehyde **1** in the presence of sodium triacetoxyborohydride. The resulting product was isolated in good yield and there was no epimerization of the lysine α proton. The Re complex was prepared in quantitative yield by adding a stoichiometric amount of [NEt$_4$]$_2$[Re(CO)$_3$Br$_3$] in methanol to compound **2**. Using these methods it is possible to produce multigram quantities of the amino acid analogue and its Re complex.

Peptide Synthesis and Characterization. Peptides were prepared on an Advanced ChemTech 348 Ω Peptide Synthesizer using HBTU as the coupling agent (Schemes 2 and 3) (*10*−*12*). The Fmoc protected dipyridyl chelate **2** and its Re complex **3**, as the bromide salt, were dissolved in DMF and coupled to the growing peptide chain using a 4-fold excess of ligand. The duration of the coupling steps to afford complete conversion to compounds **5** and **7** were determined by exposing samples of resin taken from the reaction mixtures to a solution containing ninhydrin (*13*). The time to complete conversion of the amine to the amide in both cases was identical to the conditions used for natural amino acid derivatives. As a result, modification of standard peptide coupling protocols was not necessary.

Peptides were cleaved from the resin using a TFA solution containing ethanedithiol (EDT, 2%), water (2%), and triisopropylsilane (TIS, 2%). Because of the presence of methionine, exclusion of oxygen and the use of freshly

Scheme 2. Solid-Phase Synthesis of fMLF(SAAC)G, 6

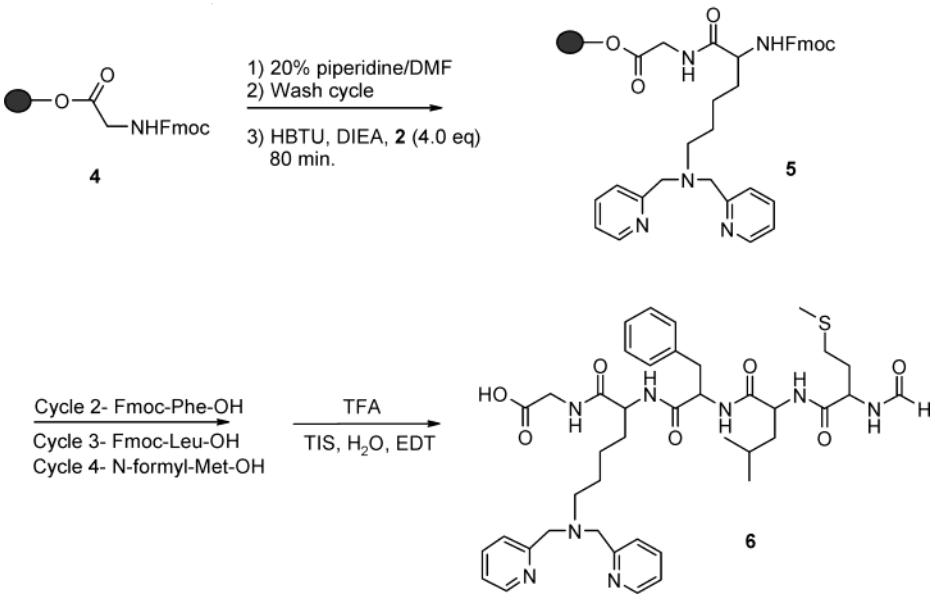

Scheme 3. Solid-Phase Synthesis of fMLF[(SAAC−Re(CO)$_3$)$^+$]G, 8

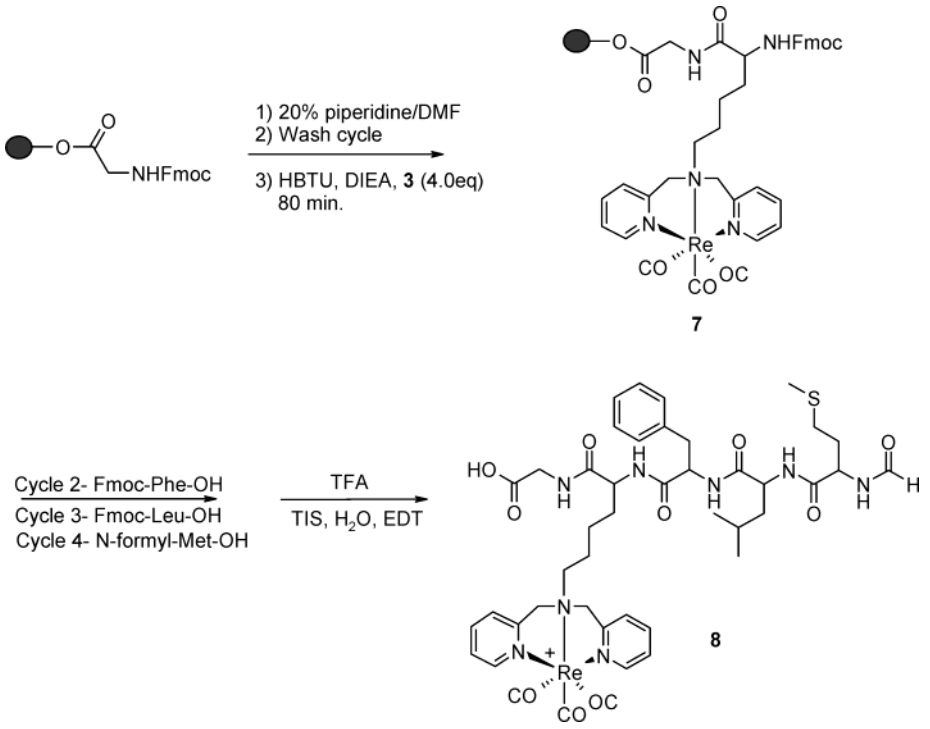

distilled EDT were necessary to avoid oxidation of the thioether to the sulfoxide. Precipitation of the peptide TFA salts was brought about by trituration with cold ether. The resulting solids were collected by centrifugation and washed with cold ether. Following dissolution in distilled water and lyophilization, compounds **6** and **8** were collected as white solids.

LCMS analysis of the crude peptide **6** showed two peaks in a 3:1 ratio. Both peaks exhibit the same *m*/*z* value (805), which corresponds to the mass of the protonated form of the desired peptide. The two components were readily separated by semipreparative HPLC and the analytical trace of the major product is shown in Figure 1a.

HPLC analysis of the crude Re complex **8** similarly showed two peaks possessing the same *m*/*z* value in the electrospray mass spectrum. Semipreparative HPLC again enabled isolation of the major product (Figure 1b), which was a colorless solid. IR analysis of **8** exhibited two distinct metal−CO stretches (1927 and 2032 cm^{-1}) which is consistent with the proposed geometry of the metal complex and similar to the values reported for the Re complex **3**.

NMR Characterization of fMLF(SAAC)G and fMLF[(SAAC−Re(CO)$_3$)$^+$]G. The ^{1}H NMR of HPLC purified **6** was run in 50/50 CF_3CO_2D−CD_3CN at 500 MHz. The spectrum (Figure 2a) shows a downfield singlet at 8.22 pm which is consistent with the presence of the formamide proton. A series of multiplets in the aromatic region were apparent, arising from the protons on the pyridine rings and the phenylalanine aryl group. The α protons of the amino acids, which appear between 4 and 5 ppm, and the side chain residues were readily assigned through the use of COSY and selective TOCSY experi-

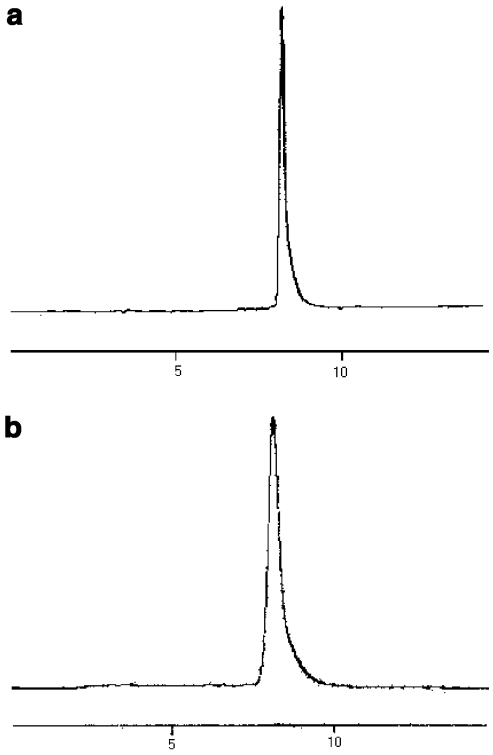

Figure 1. (a) Analytical HPLC of fMLF(SAAC)G, **6**. (b) Analytical HPLC of fMLF[(SAAC−$Re(CO)_3)^+$]G, **8**.

ments (Table 1). The α proton of the dipyridyl chelate appears at 4.37 ppm.

A comparison of the ^{1}H NMR of the Re complex (Figure 2b) with that for compound **6** shows that only the protons associated with the SAAC chelate are influenced by the presence of the Re(I) core. H-23, H-24, H-25, and H-26 shifted downfield with the latter proton moving more than one ppm (Table 1). The protons on the pyridine rings were readily assignable and shifted on average by 0.6 ppm compared to **6** with the exception of H-32 whose chemical shift, somewhat surprisingly, remained unchanged.

The ^{13}C NMR of **6** exhibited the expected number of carbonyl peaks (six) with the formamide carbon appearing at 166.1 ppm. There were numerous signals in the aromatic region corresponding to the pyridine groups and the aryl group of phenylalanine. The remainder of the peptide backbone was assigned using HSQC and HMBC spectra (Table 2).

The ^{13}C NMR of **8** showed two additional peaks downfield at 196.2 and 196.9 ppm arising from the metal−CO ligands. Two peaks are expected given the local symmetry of the complex. The remaining carbonyl groups, which are associated with the amide and acid groups of the peptide backbone, showed no major changes from that for compound **6**. Only the carbon atoms in close proximity to the Re center exhibited significant shifts. C-26 and C-27, for example, were shifted downfield to a similar degree. The carbon atoms on the pyridine groups, not surprisingly, also exhibited significant changes in chemical shift. C-30/36 shifted upfield as did C-29/35 while C-28/34 moved downfield from 154.1 to 161.3 ppm.

In Vitro Screening Studies Using Flow Cytometry. Peptides **6** and **8** were screened on a flow cytometer using a competitive binding assay (*14*−*16*) where the concentration of the competitor was allowed to vary while maintaining the concentration of the fluorescent peptide. Competitive binding data was obtained on the same day using the same blood donor as for the equilibrium binding data, to minimize variability in the number of receptors. Cells at 10^6 mL^{-1} were incubated with 1.0 nM fluorescent peptide (L) and 0.25, 0.5, 1.0, 3.0, 5.0, 10.0, and 15.0 nM competitor (U) in duplicate for 2 h at 0 °C in the dark. Flow cytometry was used to quantify the fluorescence per cell after the incubation. Neutrophils were gated on the basis of forward and side scatter parameters using Expo 32 ADC software (Beckman Coulter). The average value for nonspecific binding, obtained from the equilibrium-

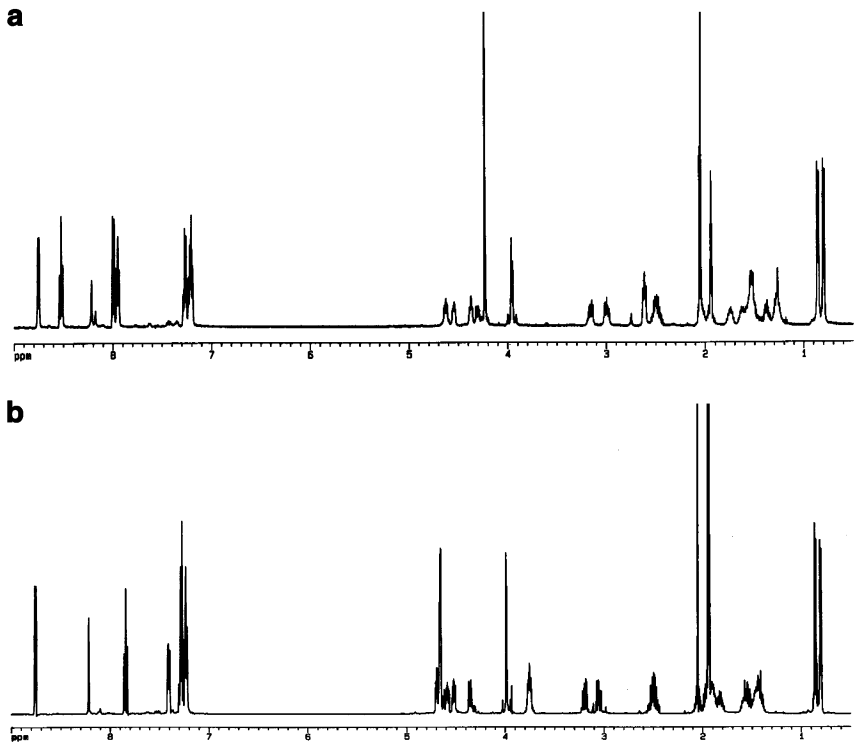

Figure 2. (a) ^{1}H NMR (500 MHz) of fMLF(SAAC)G, **6**. (b) ^{1}H NMR (500 MHz) of fMLF[(SAAC−$Re(CO)_3)^+$]G, **8**.

Table 1. ^{1}H NMR Assignments and Coupling Constants for fMLF(SAAC)G and fMLF[(SAAC−Re(CO)$_3$)$^+$]G

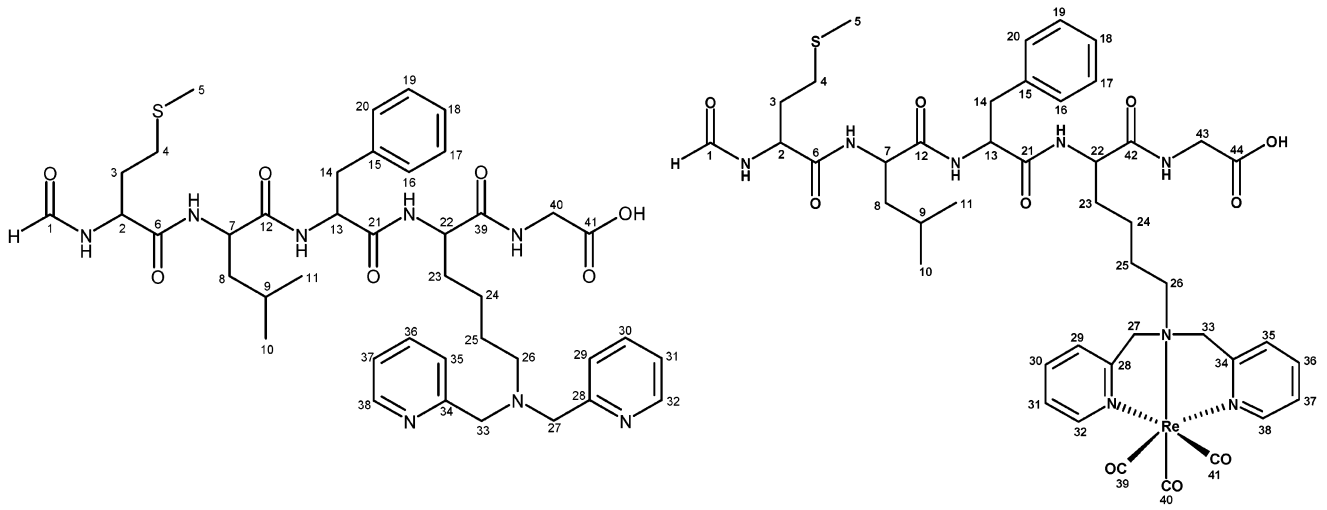

compound **6**			compound **8**		
atom label	^{1}H chemical shift (ppm)	coupling constant (Hz)	atom label	^{1}H chemical shift (ppm)	coupling constant (Hz)
1	8.220		1	8.219	
2	4.544	$^3J_{(2,3')} = 8.3$ $^3J_{(2,3'')} = 8.6$	2	4.585	$^3J_{(2,3')} = 8.6$ $^3J_{(2,3'')} = 8.7$
3′	1.951	$^2J_{(3',3'')} = -14.6$	3′	2.006	$^2J_{(3',3'')} = -11.8$
3″	2.030		3″	2.056	
4	2.484		4	2.498	
5	2.043		5	2.047	
7	4.302	$^3J_{(7,8')} = 10.4$ $^3J_{(7,8'')} = 10.2$	7	4.355	$^3J_{(7,8')} = 10.4$ $^3J_{(7,8'')} = 10.1$
8′	1.363	$^2J_{(8',8'')} = -9.2$	8′	1.424	$^2J_{(8',8'')} = -9.4$
8″	1.384		8″	1.562	
9	1.533	$^3J_{(9,10)} = 6.4$ $^3J_{(9,11)} = 6.4$	9	1.562	$^3J_{(9,10)} = 6.0$ $^3J_{(9,11)} = 6.4$
10	0.795		10	0.811	
11	0.861		11	0.904	
13	4.628	$^3J_{(13,14')} = 8.6$ $^3J_{(13,14'')} = 8.6$	13	4.697	$^3J_{(13,14')} = 5.9$ $^3J_{(13,14'')} = 5.7$
14′	2.986	$^2J_{(14',14'')} = -16.2$	14′	3.098	$^2J_{(14',14'')} = -14.0$
14″	3.155		14″	3.240	
16, 20	7.237		16−20	7.263	
17−19	7.212				
22	4.372	$^3J_{(22,23')} = 6.5$ $^3J_{(22,23'')} = 7.4$	22	4.521	$^3J_{(22,23')} = 8.6$ $^3J_{(22,23'')} = 8.4$
23′	1.528	$^2J_{(23',23'')} = -14.0$	23′	1.888	$^2J_{(23',23'')} = -9.3$
23″	1.734		23″	1.869	
24	1.271		24	1.443	
25	1.637		25	1.914	
26	2.629		26	3.753	
27/33	4.231		27/33	4.661	
29/35	7.995	$^3J_{(29,30)} = 8.0$	29/35	7.407	$^3J_{(29,30)} = 7.9$ $^3J_{(29,31)} = 3.1$
30/36	8.522	$^3J_{(30,31)} = 7.3$	30/36	7.844	$^3J_{(30,31)} = 7.9$
31/37	7.950	$^3J_{(31,32)} = 6.3$	31/37	7.263	$^3J_{(31,32)} = 5.5$
32/38	8.753		32/38 (2H)	8.759	
40	3.956	$^3J_{(40',40'')} = -5.5$	43	3.987	$^3J_{(43',43'')} = -3.0$

binding assay, was subtracted from the total fluorescence per cell when determining the ligand bound per cell. The equilibrium dissociation constant for the competing unlabeled ligand, K_d, was determined following literature procedures by fitting the specific ligand bound data to the same one-site binding model. The peptide, fMLF was used as a reference standard. Its K_d value was in good agreement with the value reported in the literature (*15*). The K_d values for fMLF and compounds **6** and **8** are given in Table 3.

DISCUSSION

To probe the utility of the single amino acid chelate (SAAC) system, derivatives of the well-studied fMLF peptide were prepared on a commercial automated peptide synthesizer. The fMLF sequence has been used to target a range of different radionuclides, including ^{99m}Tc and ^{111}In, to formyl peptide receptors (FPR) found on the surface of neutrophils as a means of imaging sites of infection and inflammation (*17*−*26*). The traditional approach to preparing these compounds has been to prepare fMLF or fMLFK sequences and to then append, in solution, a Tc ligand to the C-terminus or lysine ϵ-amine groups, respectively. In this study, the SAAC was specifically placed between a terminal glycine amino acid and the fMLF targeting sequence.

The Fmoc-dipyridyl chelate **2** and the Re complex **3** were readily incorporated into the growing peptide linked

Table 2. ^{13}C NMR Assignments for fMLF(SAAC)G and fMLF[(SAAC−Re(CO)$_3$)$^+$]G

compound 6		compound 8	
atom label	^{13}C chemical shift (ppm)	atom label	^{13}C chemical shift (ppm)
1	166.1	1	165.9
2	53.4	2	53.0
3	31.9	3	31.6
4	30.8	4	30.4
5	15.5	5	15.1
6	173.9	6	173.5
7	54.1	7	53.7
8	40.8	8	40.5
9	25.7	9	25.3
10	21.7	10	21.1
11	23.3	11	22.9
12	175.5	12	175.2
13	56.4	13	56.2
14	38.1	14	37.7
15	137.5	15	137.0
16, 20	129.9	16/17, 19/20	130.2, 129.6
17−19	130.5, 128.4	18	128.0
21	173.9	21	173.7
22	54.8	22	54.3
23	32.1	23	31.9
24	23.8	24	25.4
25	32.1	25	25.1
26	55.8	26	71.1
27/33	56.6	27/33	68.5
28/34	154.1	28/34	161.3
29/35	128.8	29/35	124.3
30/36	148.8	30/36	141.3
31/37	127.9	31/37	126.6
32/38	143.1	32/38	153.0
39	174.8	39/40/41	196.9, 196.2
40	42.2	42	174.4
41	171.8	43	41.8
		44	171.3

Table 3. Dissociation Constants

peptide	K_d (nM)
fMLF	32 ± 2.8
fMLF(SAAC)G	19 ± 3.4
fMLF[(SAAC−Re(CO)$_3$)$^+$]G	9 ± 0.8

to a SASRIN resin, using standard peptide synthesis protocols. Two products were produced in each synthesis. ^{1}H NMR showed that the minor byproducts were the result of epimeriation of the methionine α protons. To determine if the epimerization was caused by the dipyridyl ligand, the peptide was prepared using N-α-Fmoc-N-ϵ-Boc-lysine in place of compounds **2** and **3**. ^{1}H NMR again showed two sets of signals associated with the protons in the methionine backbone. Formation of the second isomer is therefore not related to the incorporation of the ligand or its Re complex but due to the ease with which *N*-formyl amino acid derivatives epimerize (*27*). When the synthesis was repeated using Fmoc-methionine in place of the *N*-formyl derivative, only one product, MLF(SAAC)G, was produced.

As the epimerization issue described previously clearly demonstrates, LCMS studies alone are not always sufficient for characterizing peptide-targeted radiopharmaceuticals. Consequently multi-NMR spectroscopy was used to fully characterize compounds **6** and **8** and to investigate the impact of Re coordination on the structure of the peptide. The ^{1}H and ^{13}C spectra of the peptide−ligand and corresponding Re complex were readily assigned using standard 2-D and selective TOCSY NMR experiments. A comparison of the ^{1}H and ^{13}C spectra for compounds **6** and **8** revealed that metal coordination does not alter the structure of the peptide backbone. The only resonances to undergo significant changes are directly associated with the SAAC. These observations suggest that radiolabeling of **6** will not cause significant structural changes. This hypothesis is supported by the in vitro studies, which showed that compound **6** and **8** have similar affinities for the FPR receptor.

Traditional radioligand displacement methods, which are not particularly suited for evaluating libraries of compounds, are typically used to screen fMLF conjugates. In this study, flow cytometric studies were undertaken as a means of evaluating ligand−receptor interactions. The advantages of using flow cytometry over traditional screening methods are that studies can be performed in real time on single cells (*14*). Flow cytometry also affords the opportunity to look at the binding of ligands to specific subpopulations. The screening studies reported here show that compounds **6** and **8** bind to granulocytes with affinities that are greater than the parent fMLF peptide, which was used as a reference standard. In light of the K_d values, compound **6** is a promising agent for targeting ^{99m}Tc to FPR receptors. Biodistribution studies in animal models of infection are currently underway.

Despite the unavoidable epimerization issue, in a single synthesis run, sufficient quantities of compounds **6** and **8** were produced to carryout characterization studies, including detailed NMR experiments, and in vitro screening studies in parallel. The chelate **2** and its Re complex behaved as typical Fmoc-amino acids and can therefore be incorporated regioselectively into any peptide using commercial peptide synthesizers. The SAAC chelate did not require any additional protecting groups beyond the N-α-Fmoc group, and its metal complex was stable to the conditions used to prepare the peptide and cleave it from the support. The ability to prepare macroscopic quantities of the metal complex, which exists as a single isomer, offers a tremendous advantage over other more commonly employed Tc ligand systems such as HYNIC where purification and detailed characterization of the ^{99}Tc and Re complexes are habitually problematic.

The commercial viability of the [Tc(CO)$_3$]$^+$ core as a synthon for the preparation of radiopharmaceuticals has been queried recently (*28*). Despite the numerous benefits of working with Tc(I), which have been elegantly summarized by Alberto (*29*) and highlighted throughout this paper, intellectual property issues and the increasing clinical use of PET in the United States have brought into question as to whether a clinically useful agent based on the Tc-carbonyl motif will ever be realized.

The current widespread use of technetium in nuclear medicine is not driven solely by the advantages of working with ^{99m}Tc, but by the clinical usefulness of ^{99m}Tc radiopharmaceuticals. The discovery of new imaging agents will determine the future role of ^{99m}Tc in diagnostic nuclear medicine, as is the case for all radionuclides, which places considerable importance on developing new methods that can improve the efficiency of the radiopharmaceutical discovery process. It should also be noted that the opportunity to prepare complementary (i.e. isostructural) Re radiotherapy agents based on ^{186}Re and ^{188}Re will further enhance the future demand for new Tc radiopharmaceuticals.

To develop new Tc and Re radiopharmaceuticals in a reasonable time frame and in a cost-effective manner, researchers must shift to more contemporary drug discovery techniques, like the strategy reported here. Because the Tc(I) and Re(I) core is highly versatile and much more amenable to modern drug discovery techniques than existing Tc/Re (or other radiometal) synthons, commercial matters aside, there is a high prob-

ability that clinically viable diagnostic and/or therapeutic agent based on the Tc(I) or Re(I) carbonyl cores will be discovered.

CONCLUSIONS

The single amino acid chelate used in this study affords the opportunity to incorporate a Tc(I)/Re(I) binding ligand into peptides using standard solid-phase synthesis methods. The derivatization strategy is flexible in that it allows for the chelate to be incorporated at any position in the peptide as an additional amino acid or in place of an existing amino acid that is not involved in receptor binding. In the present study, novel derivatives of a simple chemotactic peptide were prepared and screened using flow cytometry. The use of flow cytometry as a screening strategy creates the opportunity to rapidly identify compounds that are capable of selectively targeting specific types of granulocytes. The focus of our current efforts is to build upon the reported synthesis and screening methods to develop and screen combinatorial libraries of compounds that are capable of targeting specific cell populations that accumulate at sites of infection and inflammation.

ACKNOWLEDGMENT

We thank The Canadian Foundation for Innovation (CFI) and The Ontario Innovation Trust (OIT) and McMaster University for providing the infrastructure used in this project and NSERC of Canada for a scholarship for K.A.S..

Supporting Information Available: HPLC, ESMS, ^{1}H and ^{13}C NMR, FT-IR data, and competetive binding data. This material is available free of charge via the Internet at http://pubs.acs.org.

LITERATURE CITED

(1) Liu, S., and Edwards, D. S. (1999) ^{99m}Tc-Labeled small peptides as diagnostic radiopharmaceuticals. *Chem. Rev. 99*, 2235−2268.

(2) Fischman, A. J., Babich, J. W., and Strauss, H. W. (1993) A ticket to ride: peptide radiopharmaceuticals. *J. Nucl. Med. 34*, 2253−2263.

(3) Valliant, J. F., Riddoch, R. W., Hughes, D. W., Roe, D. G., Fauconnier, T. K., and Thornback, J. R. (2001) The solid-phase synthesis and NMR spectroscopy of a ^{99}Tc chelate-bombesin derived peptide conjugate. *Inorg. Chim. Acta 325*, *155*-163.

(4) Smith, C. J., Gali, H., Sieckman, G. L., Higginbotham, C., Volkert, W. A., and Hoffman, T. J. (2003) Radiochemical investigations of ^{99m}Tc−N_3S−X-BBN[7−14]NH_2. An in vitro/in vivo structure−activity relationship study where $X = 0$, 3, 5, 8, and 11-carbon tethering moieties. *Bioconjugate Chem. 14*, 93−102.

(5) Gariépy, J., Rémy, S., Zhang, X., Ballinger, J. R., Bolewska,-Pedyczak, E., Rauth, M., and Bisland, S. K. (2002) A simple two-step approach for introducing a protected diaminedithiol chelator during solid-phase assembly of peptides. *Bioconjugate Chem. 13*, 679−684.

(6) Greenland, W. E. P., Howland, K., Hardy, J., Fogelman, I., and Blower, P. J. (2003) Solid-phase synthesis of peptide radiopharmaceuticals using Fmoc-N-ϵ-(HYNIC−Boc)-lysine, a technetium-binding amino acid: application to Tc-99m-labeled salmon calcitonin. *J. Med. Chem. 46*, 1751−1757.

(7) Hunter, D. H., and Luyt, L. G. (2000) Lysine conjugates for the labeling of peptides with technetium-99m and rhenium. *J. Labelled Compd. Radiopharm. 43*, 403−412.

(8) Banerjee, S. R., Levadala, M. K., Lazarova, N., Wei, L., Valliant, J. F., Stephenson, K. A., Babich, J. W., Maresca, K. P., and Zubieta, J. (2002) Bifunctional single amino acid chelates (SAAC) for labeling of biomolecules with $\{Tc(CO)_3\}^{+1}$ and $\{Re(CO)_3\}^{+1}$ cores. The crystal and molecular structures of $[ReBr(CO)_3(H_2NCH_2C_5H_4N)]$, $[Re(CO)_3\{X(Y)NCH_2CO_2-CH_2CH_3\}]Br$, (X ═Y= 2-pyridylmethyl; X = 2-pyridylmethyl, Y = 2-(1-methylimidazolyl)methyl; X ═Y= 2-(1-methylimidazolyl)methyl, $[ReBr(CO)_3\{(C_5H_4NCH_2)NH(CH_2C_4H_3S)]$ and $[Re(CO)_3\{(C_5H_4NCH_2)N(CH_2C_4H_3S)CH_2CO_2)]$. *Inorg. Chem. 41*, 6417−6425.

(9) Levadala, M. K, Banerjee, S. R., Babich, J. W., and Zubieta, J. Sodium triacetoxyborohydride: A robust reagent for direct reductive alkylation of amino acids. Applications for the synthesis of bifunctional chelates for nuclear imaging. Unpublished results.

(10) Chan, W. C., and White, P. D. *FMOC Solid-Phase Peptide Synthesis, A Practical Approach*; Oxford University Press: New York, 2000.

(11) Fields, G. B., and Noble, R. L. (1990) Solid-phase peptide synthesis utilizing 9-fluorenylmethoxycarbonyl amino acids. *Int. J. Pept. Protein. Res. 35*, 161−214.

(12) Fields, C. G., Lloyd, D. H., Macdonald, R. L., Otteson, K. M., and Noble, R. L. (1991) HBTU Activation for automated Fmoc solid-phase peptide synthesis. *Pept. Res. 4*, 95−101.

(13) Sarin, V. K., Kent, S. B., Tam, J. P., and Merrifield, R. B. (1981) Quantitative monitoring of solid-phase peptide synthesis by the ninhydrin reaction. *Anal. Biochem. 117*, 147−157.

(14) Waller, A., Pipkorn, D., Sutton, J. L., Linderman, J. L., and Omann, G. M. (2001) Validation of flow cytometric competitive binding protocols and characterization of fluorescently labeled ligands. *Cytometry 45*, 102−114.

(15) Fay, S. P., Posner, R. G., Swann, W. N., and Sklar, L. A. (1991) Real-Time analysis of the assembly of ligand, receptor, and G protein by quantitative fluorescence flow cytometry. *Biochemistry 30*, 5066−5075.

(16) Hoffman, J. F., Keil, M. L., Riccobene, T. A., Omann, G. M., and Linderman, J. L. (1996) Interconverting receptor states at 4 °C for the neutrophil N-formyl peptide receptor. *Biochemistry 35*, 13047−13055.

(17) Babich, J. W., Graham, W., Barrow, S. A., Dragotakes, S. C., Tompkins, R. G., Rubin, R. H., and Fischman, A. J. (1993) Technetium-99m-labeled Chemotactic Peptides: Comparison with indium-111-labeled white blood cells for localizing acute bacterial infection in the rabbit. *J. Nucl. Med. 34*, 2176−2181.

(18) Van Der Laken, C. J., Boerman, O. C., Oyen, W. J. G., Van Der Ven, M. T. P., Edwards, D. S., Barrett, J. A., Van Der Meer, J. W. M., and Corstens, F. H. M. (1997) Technetium-99m-labeled chemotactic peptides in acute infection and sterile inflammation. *J. Nucl. Med. 38*, 1310−1315.

(19) Edwards, D. S., Liu, S., Ziegler, M. C., Harris, A. R., Crocker, A. C., Heminway, S. J., Barrett, J. A., Bridger, G. J., Abrams, M. J., and Higgins, J. D., III. (1999) RP463: A stabilized technetium-99m complex of a hydrazino nicotinamide derivatized chemotactic peptide for infection imaging. *Bioconjugate. Chem. 10*, 884−891.

(20) Babich, J. W., Coco, W. G., Barrow, S., Fischman, A. J., Femia, F. J., and Zubieta, J. (2000) 99mTc-labeled chemotactic peptides: influence of coligand on distribution of molecular species and infection imaging properties. Synthesis and structural characterization of model complexes with the $\{Re(^2\text{-}HNNC_5H_4N)(^1\text{-}NNC_5H_4N)\}$ core. *Inorg. Chim. Acta 309*, 123−136.

(21) Babich, J. W., Graham, W., Barrow, S. A., and Fischman, A. J. (1995) Comparison of the infection imaging properties of a ^{99m}Tc labeled chemotactic peptide with ^{111}In IgG. *Nucl. Med. Biol. 22*, 643−648.

(22) Fischman, A. J., Pike, M. C., Kroon, D., Fucello, A. J., Rexinger, D., TenKate, C., Wilkinson, R., Rubin, R. H., and Strauss, H. W. (1991) Imaging focal sites of bacterial infection in rats with indium-111-labeled chemotactic peptide analogs. *J. Nucl. Med. 32*, 483−491.

(23) Rennen, H. J., Corstens, F. H., Oyen, W. J., and Boerman, O. C. (2001) New concepts in infection/inflammation imaging. *Quart. J. Nuc. Med. 45*, 167−173.
(24) Verbeke, K., Verbeke, A., Vanbilloen, H., and Verbruggen, A. (2002) Preparation and preliminary evaluation of ^{99m}Tc-EC−For-MLFK. *Nucl. Med. Biol. 29*, 585−592.
(25) Baidoo, K. E., Scheffel, U., Stathis, M., Finley, P., Lever, S. Z., Zhan, Y., and Wagner, H. N., Jr. (1998) High-affinity no-carrier-added ^{99m}Tc-labeled chemotactic peptides for studies of inflammation in vivo. *Bioconjugate Chem. 9*, 208−217.
(26) Babich, J. W., Solomon, H., Pike, M. C., Kroon, D., Graham, W., Abrams, M. J., Tompkins, R. G., Rubin, R. H., and Fischman, A. J. (1993) Technetium-99m-labeled hydrazino nicotinamide derivatized chemotactic peptide analogues for imaging focal sites of bacterial infection. *J. Nucl. Med. 34*, 1964−1974.
(27) Greathouse, D. V., Goforth, R. L., Crawford, T., Van der Wel, P. C., and Killian, J. A. (2001) Optimized aminolysis conditions for cleavage of N-protected hydrophobic peptides from solid-phase resins. *J. Pept. Res. 57*, 519−527.
(28) Welch, M. J., and Lewis, J. S. (2003) $[Tc(CO)_3]^+$ chemistry: a promising new concept for SPECT? *Eur. J. Nucl. Med. 30*, 1302−1304.
(29) Alberto, R. (2003) $[Tc(CO)_3]^+$ chemistry: a promising new concept for SPET? *Eur. J. Nucl. Med. 30*, 1299−1302.

BC034128S